Supplementary Figures

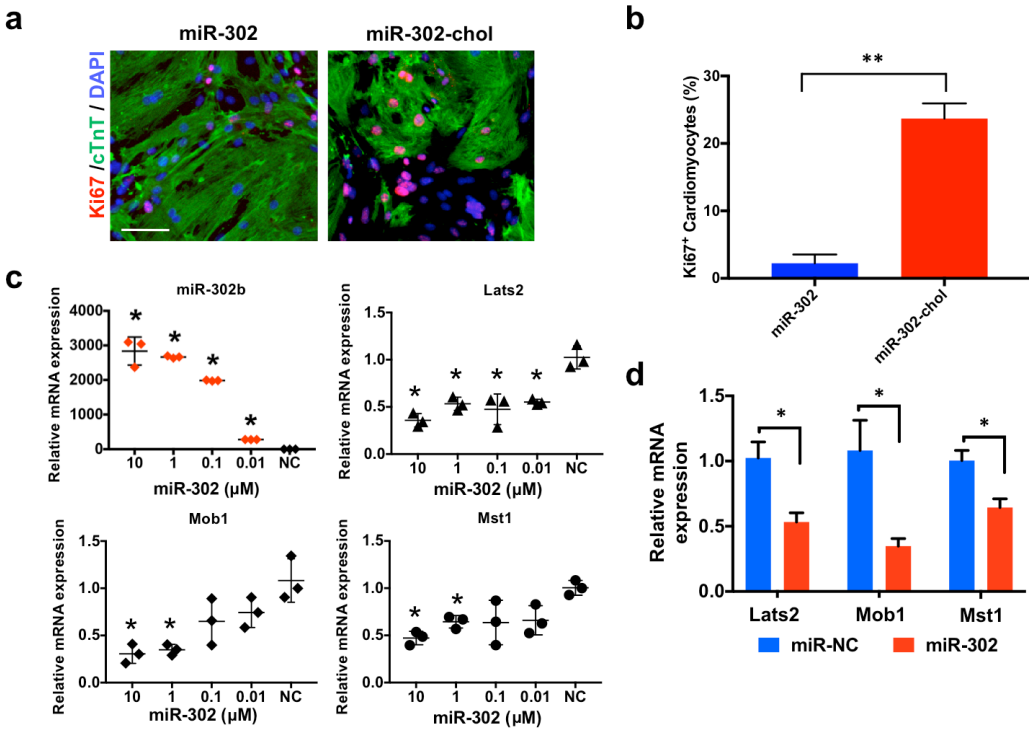

Supplementary Figure 1. **Cholesterol-modification of miR-302 mimics**. Proliferation of neonatal mouse cardiomyocytes by un-modified (miR-302) and cholesterol modified (miR-302-chol) miR-302b/c mimics (200 μM), using a) co-staining and b) quantification of cTnT and Ki67 to denote cardiomyocyte proliferation. Cardiomyocytes were treated with miR-302 for 24 hours; staining was performed after 48 hours. Quantification was based on counting of $Ki67^{+}cTnT^{+}$ co-stained cells relative to total $cTnT^{+}$ cells per HPF. Scale bar = 50 μm (mean ± SD, n=3, **p<0.01). c) qPCR quantification of miR-302b, Lats2, Mob1, and Mst1 in neonatal cardiomyocytes following dose response to miR-302-chol demonstrates a dose dependent knockdown of Hippo components to concentrations as high as 10 μm (mean ± SD, n=3, *p<0.05 compared to miR-NC). d) Quantification of miR-302 knockdown by qPCR at 1 μm (mean ± SD, n=3, *p<0.05 compared to miR-NC).

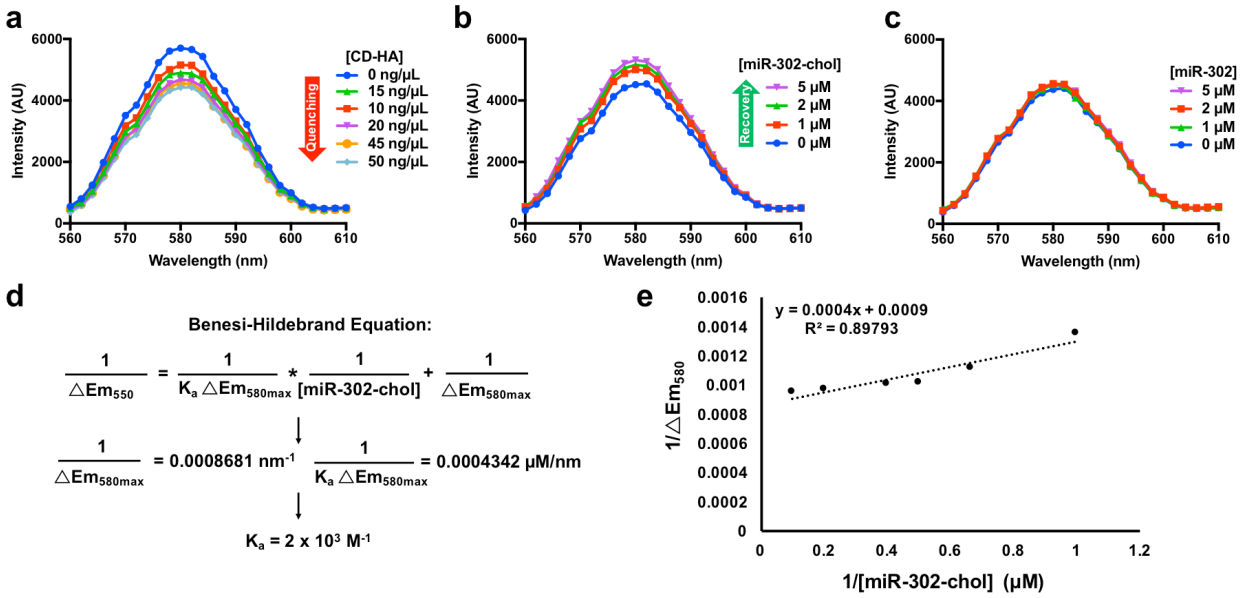

Supplementary Figure 2. miR-302-chol interaction with CD-HA. a) Rhodamine B fluorescence is quenched by CD-HA due to hydrophobic interaction. Increasing amounts of CD-HA saturate quenching at 50 ng/μL. b) At a saturating concentrating of CD-HA (50 ng/μL), cholesterol-modified miR-302 interacts with CD-HA/Rho B complexes to displace and unquench rhodamine, recovering fluorescence in a dose-dependent fashion. c) Unmodified miR-302 does not lead to fluorescent recovery of CD-HA/Rho B complexes. d) The Benesi-Hildebrand equation can be used to determine the binding constant between the cholesterol-modified mimic and CD-HA, which approximates the guest-host binding affinity. At each dose of miR-302-chol, the change in fluorescence (ΔEm_{580}) is calculated and plotted as $1/(\Delta Em_{580})$ on the y-axis and 1/[miR-302-chol] on the x-axis. e) The y-intercept of the best-fit line allows for the calculation of $\Delta Em_{580}max$, which was used to calculate the K_a value from the slope $[1/(K_a*\Delta Em_{580}max)]$.

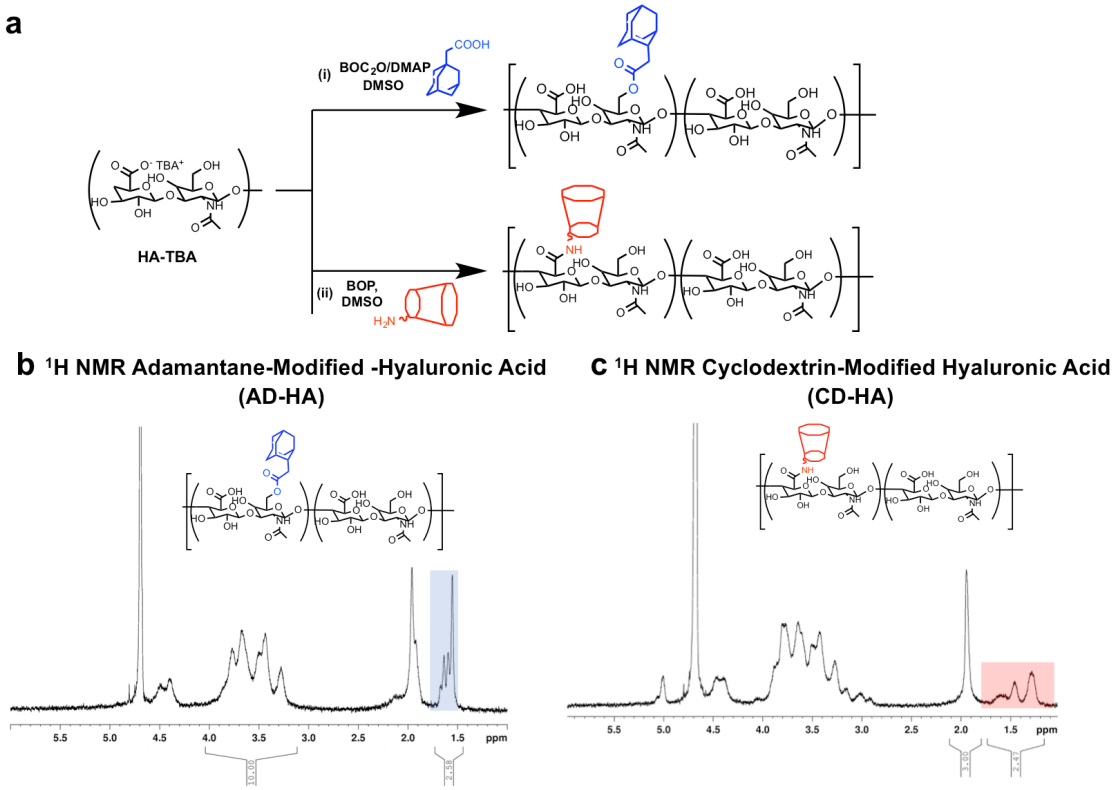

Supplementary Figure 3. Synthesis and ^{1}H NMR Spectra of AD-HA and CD-HA. a) AD-HA was synthesized from the esterification between 1-adamantaneacetic acid and the primary alcohol of HA by di-tert-butyl dicarbonate (Boc_2O). CD-HA was synthesized from the amidation reaction between aminated cyclodextrin (mono-(6-hexanediamine-6-deoxy)-β-cyclodextrin) and the carboxylic acid of HA by (benzotriazol-1-yloxy)tris(dimethylamino)phosphonium hexafluorophosphate (BOP).[1] b) Adamantane functionalization was determined to be ~20% from integration of the ethyl multiplet of adamantane (δ=1.42-1.70, 12 H) relative to the HA backbone (δ=3.10-4.10, 10 H). c) Cyclodextrin functionalization was determined to be ~20% by integration of the hexane linker (δ=1.22-1.77, 12 H) relative to the methyl singlet of HA (δ=2.1, 3 H).

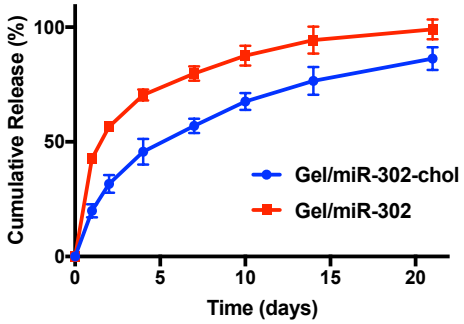

Supplementary Figure 4. Release of cholesterol-modified and un-modified miR-302. Gels (100 µL, 5 wt%) were assembled with either cholesterol-modified or unmodified miR-302 (210 µM of miR-302b and 210 µM of miR-302c). PBS was added above gels in microcentrifuge tubes and collected serially over three weeks to quantify total miR-302 release. At 21 days, gels were dissolved in adamantane solution to determine the remaining miR-302 and all values were normalized to the cumulative miR-302. miR-302 release was slower when modified with cholesterol due to complexes between cholesterol and CD (mean ± SD, n=3 gels per group).

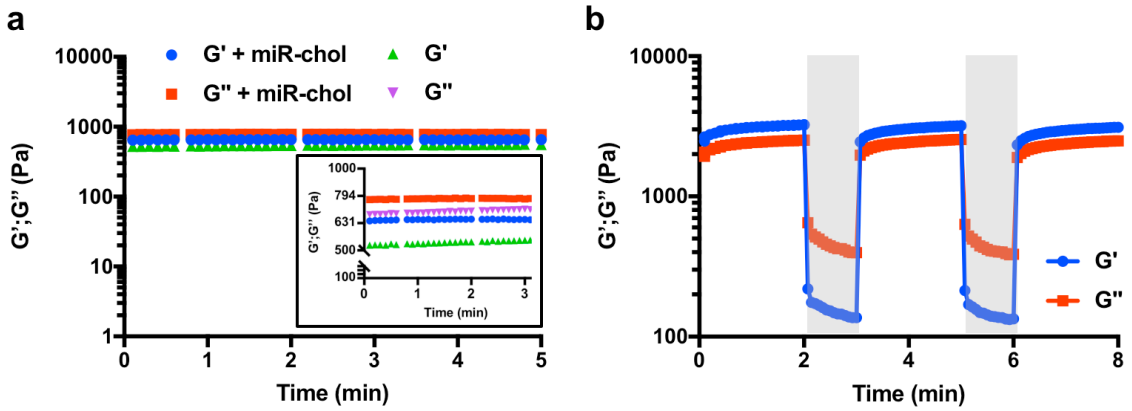

Supplementary Figure 5. Shear oscillatory rheology of hydrogels with encapsulated miR-302-chol. a) Time sweep of storage (G') and loss (G'') moduli (1 Hz, 0.5% strain) of gels (5 wt%) alone or with encapsulated miR-302 (210 μM of miR-302b and 210 μM of miR-302c). miR-302 inclusion minimally affects moduli. b) Alternating low (0.5%) and high (250%, gray shading) strain (20 Hz, 0.5% strain) of hydrogel complexes. G' declines below G'' in response to high strain, indicating flow and predominant liquid properties (G''>G') at high strains. Upon cessation of strain, G' and G'' recover to initial mechanics (G'>G'').

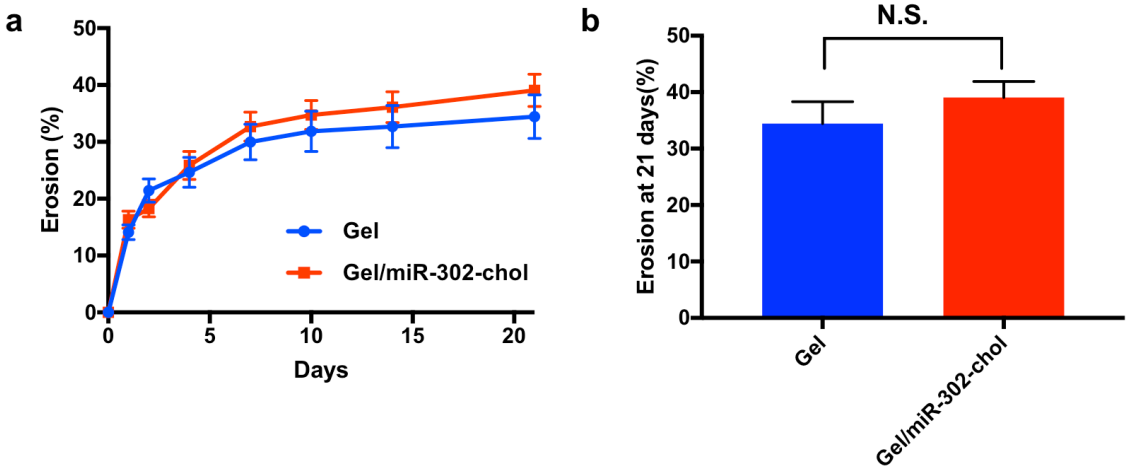

Supplementary Figure 6. **Hydrogel erosion**. a) Gels (100 μL) were formed with or without miR-302 (210 μM of miR-302b and 210 μM of miR-302c) at 5 wt% in microcentrifuge tubes. PBS was added to gels, collected over three weeks, and quantified for hyaluronic acid content through a uronic acid colorimetric assay. b) Erosion by three weeks indicated minimal difference when the miR-302 was included (mean ± SD, n=3, N.S. = not significant).

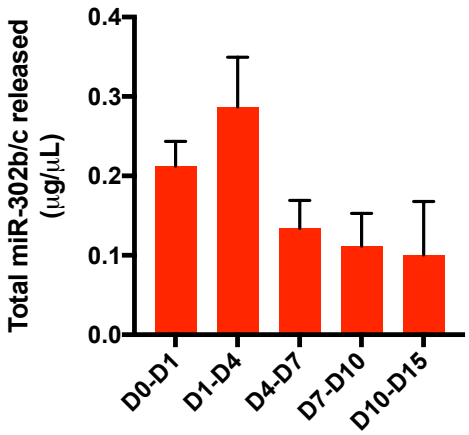

Supplementary Figure 7. Absolute miR-302 release from gels at various intervals. Release of gel/miR-302-chol expressed as total miR-302 concentration. Release from D0-D1, D1-D4, D4-D7 correspond to approximate concentrations of ~5-10 μM miR-302 in releasate solution that is subsequently added to neonatal cardiomyocytes for proliferation assays (mean ± SD, n=3). Exact concentrations of miR-302 (μM) expressed in releasates were as follows: D0-D1 = 7.5 μM, D1-D4=10.2 μM, D4-D7=4.9 μM, D7-D10 = 4.0 μM, D10-D15 = 3.6 μM.

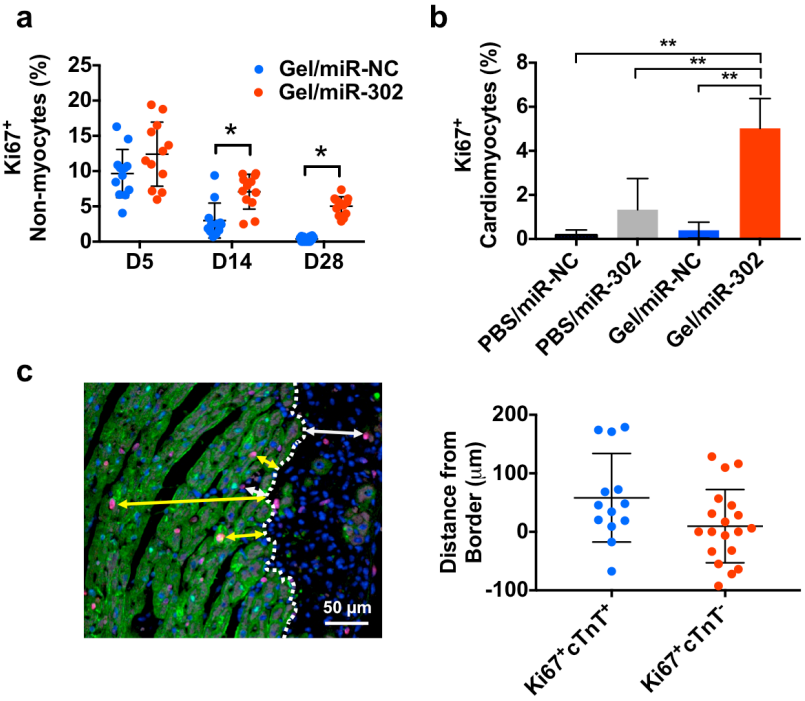

Supplementary Figure 8. *In vivo* cell proliferation. a) Mice were selected receive miR-302 or miR-NC (2x5 μL) injections with gel or PBS in non-infarcted heart tissue inferior and lateral to the LAD at the left atrial appendage. At 5, 14, or 28 days, hearts were sectioned and stained for Ki67. Quantification of Ki67 non-myocytes (Ki67+cTnT-) in HPFs was performed around both injection sites for three mice per group (mean ± SD, n=3 mice per group, *p<0.05). b) Quantification of Ki67+ cardiomyocytes ($Ki67^+cTnT^+$) in HPFs surrounding injection sites at D5, demonstrating increased proliferation from gel/miR-302 compared to all controls (mean ± SD, n=3 mice per group, **p<0.01). c) In gel/miR-302 treated sections, proliferating cells were quantified from the injection border, where distance away from injection site (toward $cTnT^+$ area) is positive and distance into injection site (toward $cTnT^-$ area) is negative. Yellow and white arrows indicate representative proliferating cardiomyocytes ($Ki67^+cTnT^+$) and non-myocytes ($Ki67^+cTnT^-$) surrounding injection site (mean ± SD, n=3 mice).

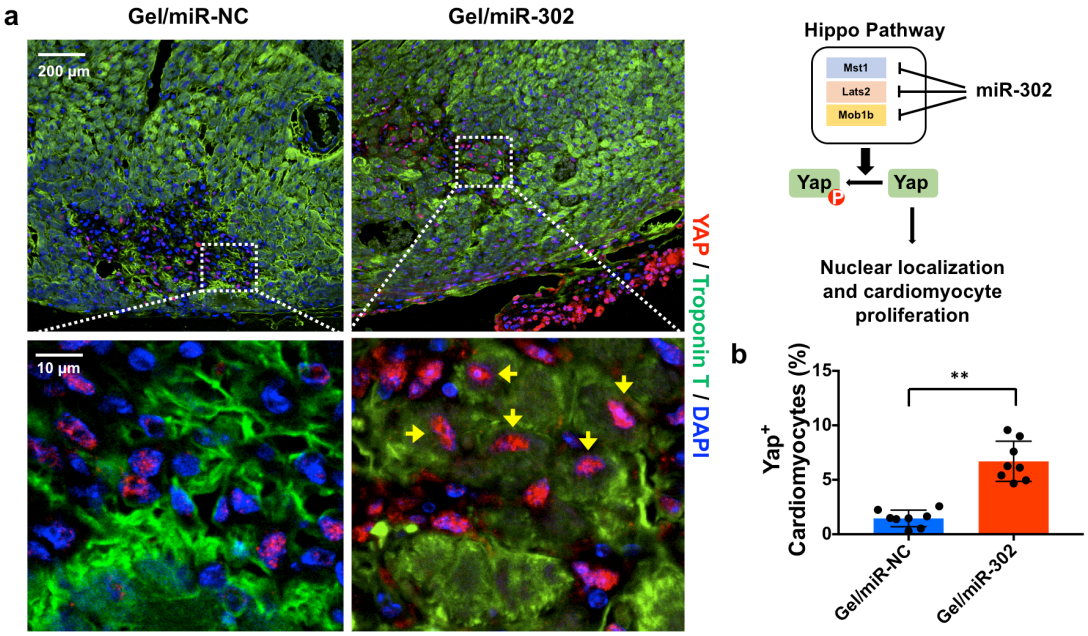

Supplementary Figure 9. Yap expression. Two gel/miR-302 injections were made inferolateral to the proximal LAD without ligation of the LAD in mice. a) Sections were co-stained with Yap after five days post treatment with gel/miR-NC or gel/miR-302. Yap localizes to the nucleus in response to miR-302 stimulation to interact with TEAD transcription factors to cause cardiomyocyte proliferation.[2] b) Quantification of Yap in HPFs surrounding both injection sites for a minimum of three mice per group. Sections demonstrate increased total nuclear Yap (yellow arrows) in gel/miR-302 treated groups (mean ± SD, n=3 mice per group, **p<0.01.)

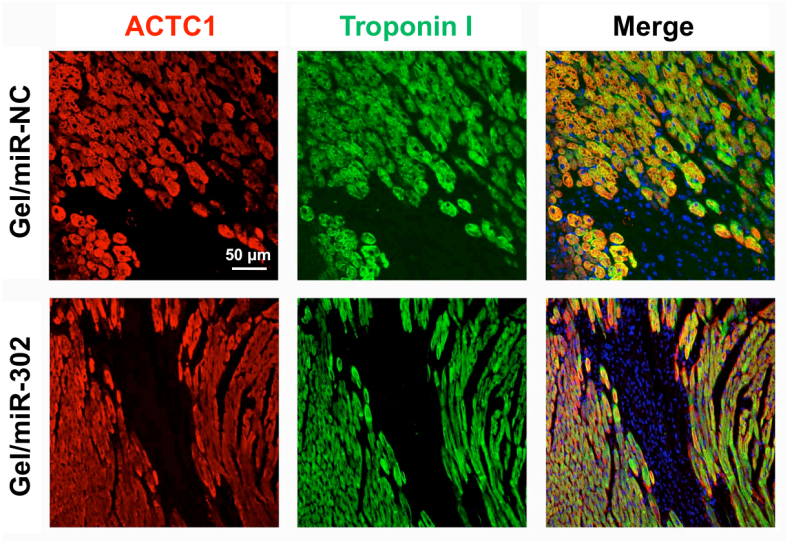

Supplementary Figure 10. Cardiomyocyte maturity staining. Two gel/miR-302 injections were made inferolateral to the proximal LAD without ligation of the LAD in mice. Sections were co-stained with cardiac muscle α-actin (ACTC1) and cardiac Troponin I after five days post treatment with gel/miR-NC or gel/miR-302. ACTC1 is a marker of cardiomyocytes during all stages of maturation (including immaturity) whereas Troponin I stains only mature cardiomyocytes. Complete overlap of the two cardiac markers suggests retention of a mature phenotype following gel/miR-302 injection.

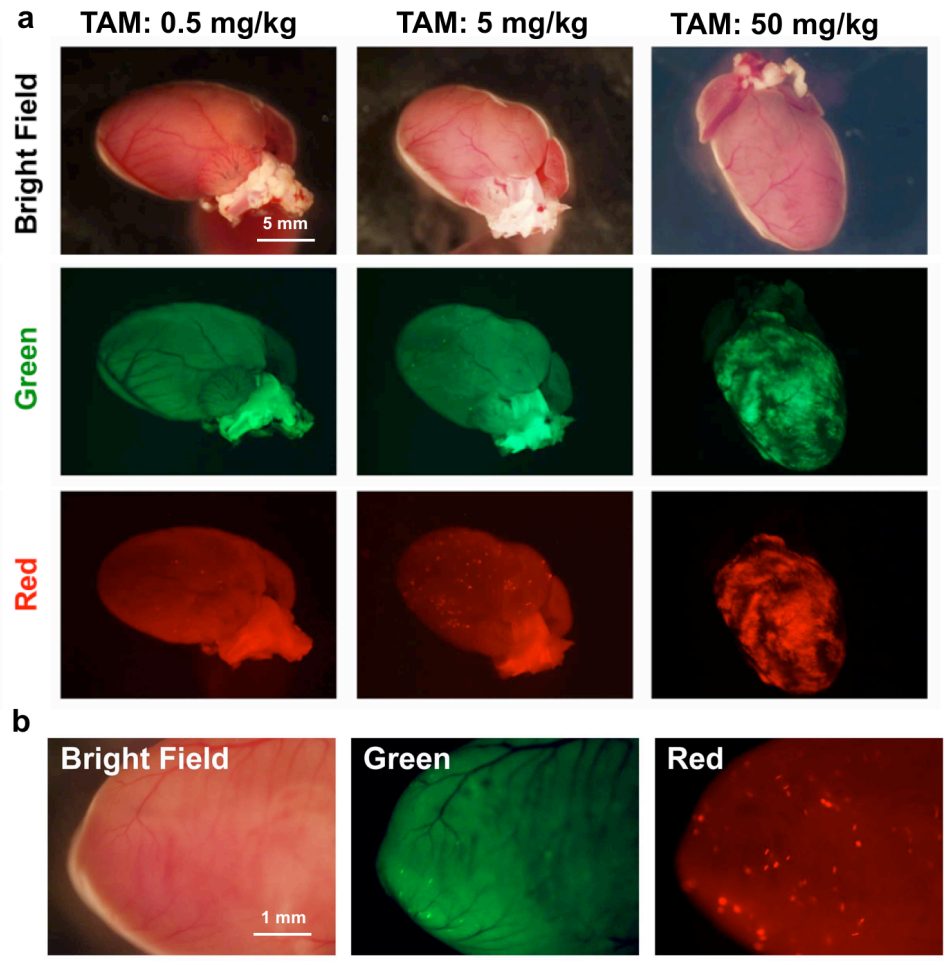

Supplementary Figure 11. Confetti hearts prior to ligation or gel injection. a) Tamoxifen titration indicates increasing GFP and RFP reporter expression with increasing tamoxifen induction. b) Representative gross image of MHC-Confetti heart in green and red channels following Tamoxifen induction of reporter expression for 14 days but prior to gel/miR-302 injection.

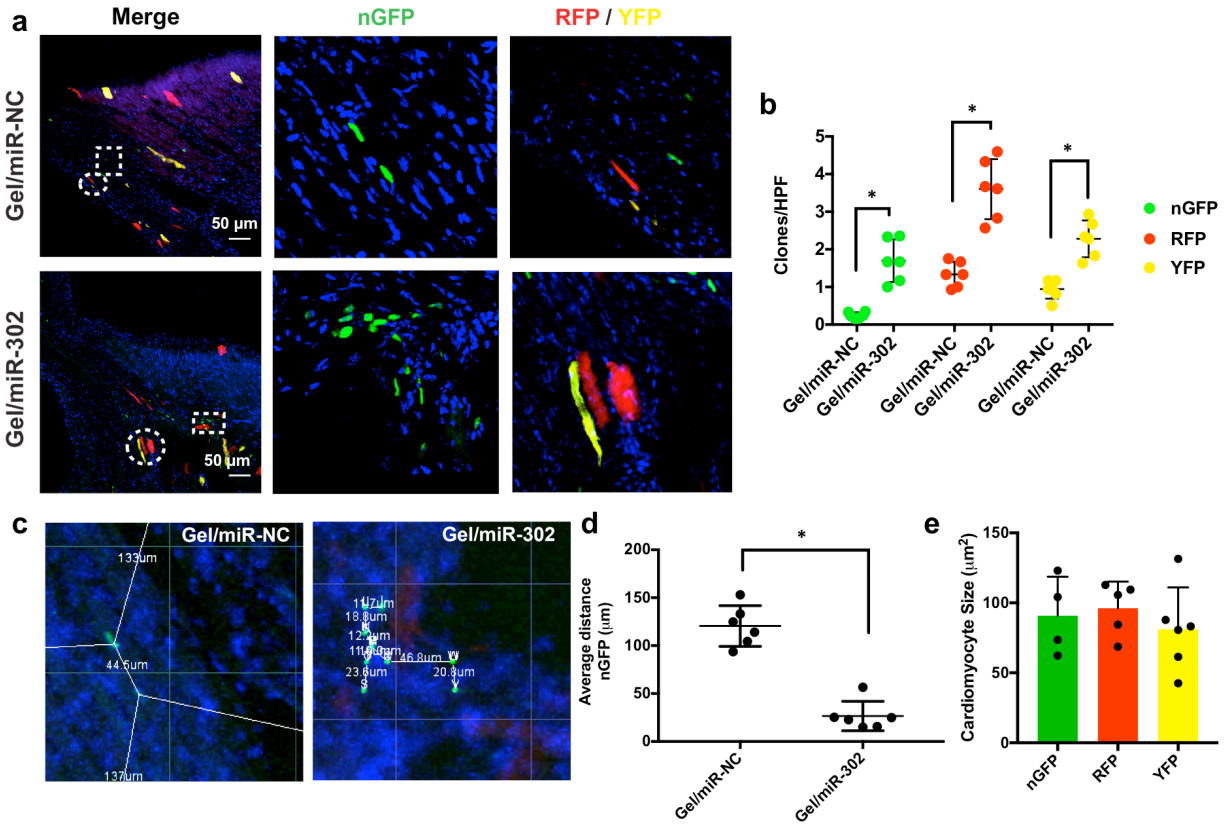

Supplementary Figure 12. Clonal proximity in hearts injected with gel/miR-NC compared to gel/miR-302. a) Fluorescently-labeled cells were identified in border zones of infarcts with clones neighboring each other in gel/miR-302 treated sections. Neighboring nGFP, RFP and YFP cells are magnified to demonstrate clones. b) Quantification of clones suggesting increased clones in gel/miR-302 treated groups for all three fluorescent reporter proteins. A clone is defined as a minimum of two neighboring cells within 50 µm of each other. (mean ± SD, gel/miR-NC, n=3; gel/miR-302, n=4, *p<0.05) c) nGFP cells were found within 50 µM of each other gel/miR-302 sections, whereas they were greater than 100 µM apart in gel/miR-NC sections. Measurements were performed by IMARIS from 3D confocal images. d) Quantification of distance between neighboring nGFP cells from IMARIS measurements (mean ± SD, gel/miR-NC, n=3; gel/miR-302, n=4, *p<0.05). e) Quantification of cardiomyocyte size in each of nGFP, RFP, and YFP channels using WGA to observe cardiomyocyte membranes. No evidence for hypertrophy was observed (mean ± SD, gel/miR-NC, n=3; gel/miR-302, n=4).

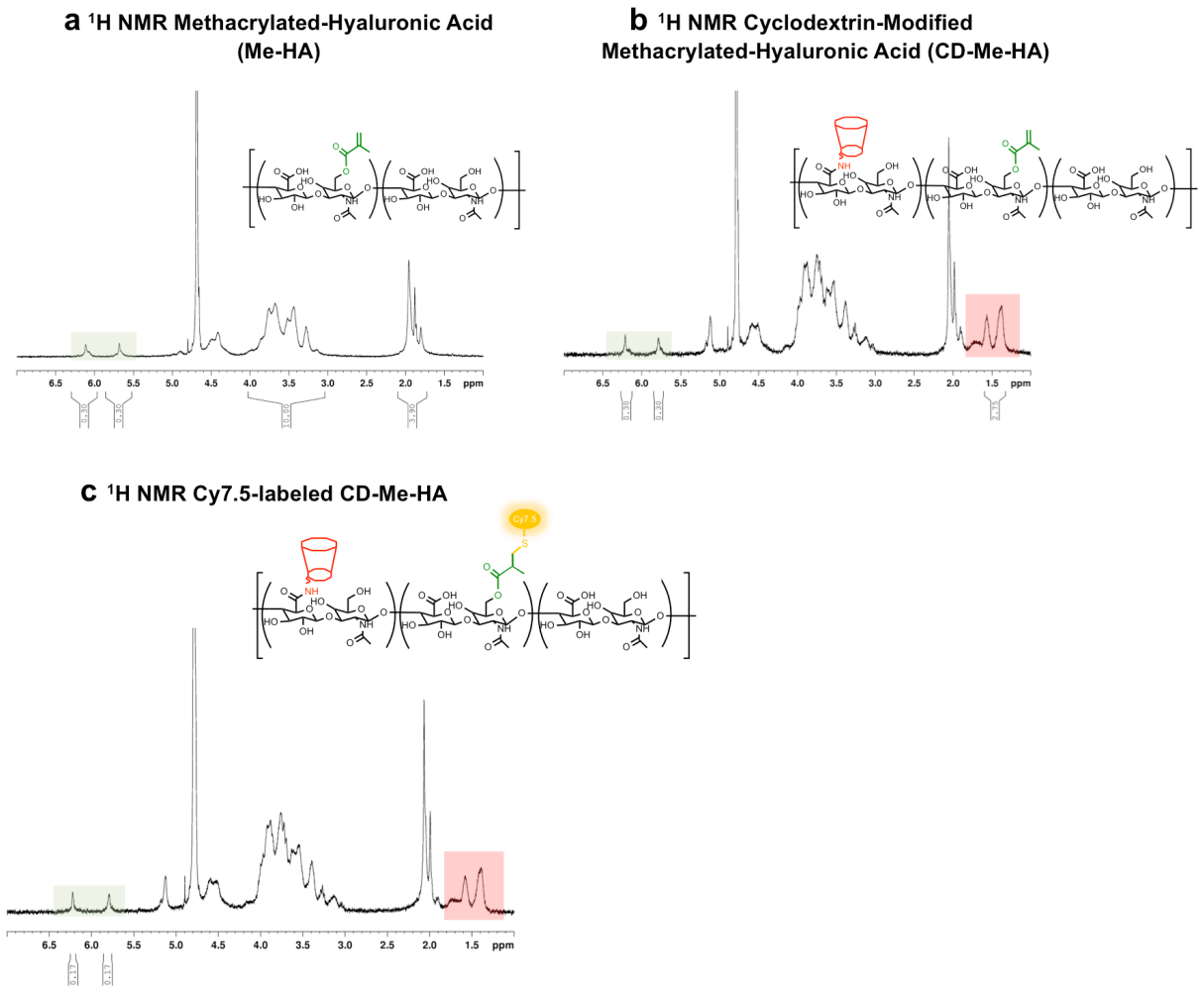

Supplementary Figure 13. ^{1}H NMR Spectra of Me-HA, CD-Me-HA, and Cy7.5-labeled CD-Me-HA. Me-HA was synthesized as previously described.[3] a) Methacrylate functionalization was determined to by ~30% by integration of methacrylate alkene protons (δ=5.5-6.5, 2 H) relative to the methyl singlet of HA (δ=2.1, 3 H). b) CD-Me-HA was synthesized was previously described through by formation of the TBA salt and subsequent amidation reaction between aminated cyclodextrin (mono-(6-hexanediamine-6-deoxy)-β-cyclodextrin) and the carboxylic acid of HA by (benzotriazol-1-yloxy)tris(dimethylamino)phosphonium hexafluorophosphate (BOP). Cyclodextrin functionalization on Me-HA was determined to be ~20% by integration of the hexane linker (δ=1.22-1.77, 12 H) relative to the alkene protons of methacrylate (δ=5.5-6.5, 2 H). c) Cy7.5-labeling of CD-Me-HA was performed through a Michael addition reaction between a thiolated Cy7.5 peptide (GCKKG-Cy7.5) and CD-Me-HA at pH 8 as previously described.[3] Functionalization of CD-Me-HA with Cy7.5 was determined by integrating the alkene protons of methacrylate (δ=5.5-6.5, 2 H) relative to the hexane linker of CD-HA (δ=1.22-1.77, 12 H). The reduction in alkene protons suggests an approximate modification Cy7.5 modification of 13% of disaccharides in CD-Me-HA.

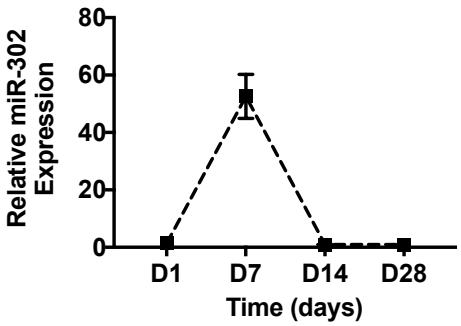

Supplementary Figure 14. miR-302 expression in the lungs. qPCR quantification of miR-302 in the lungs at various timepoints following gel/miR-302 and MI, normalized to gel/miR-NC, indicating minimal miR-302 expression in lungs (mean ± SD, n=3 mice per timepoint).

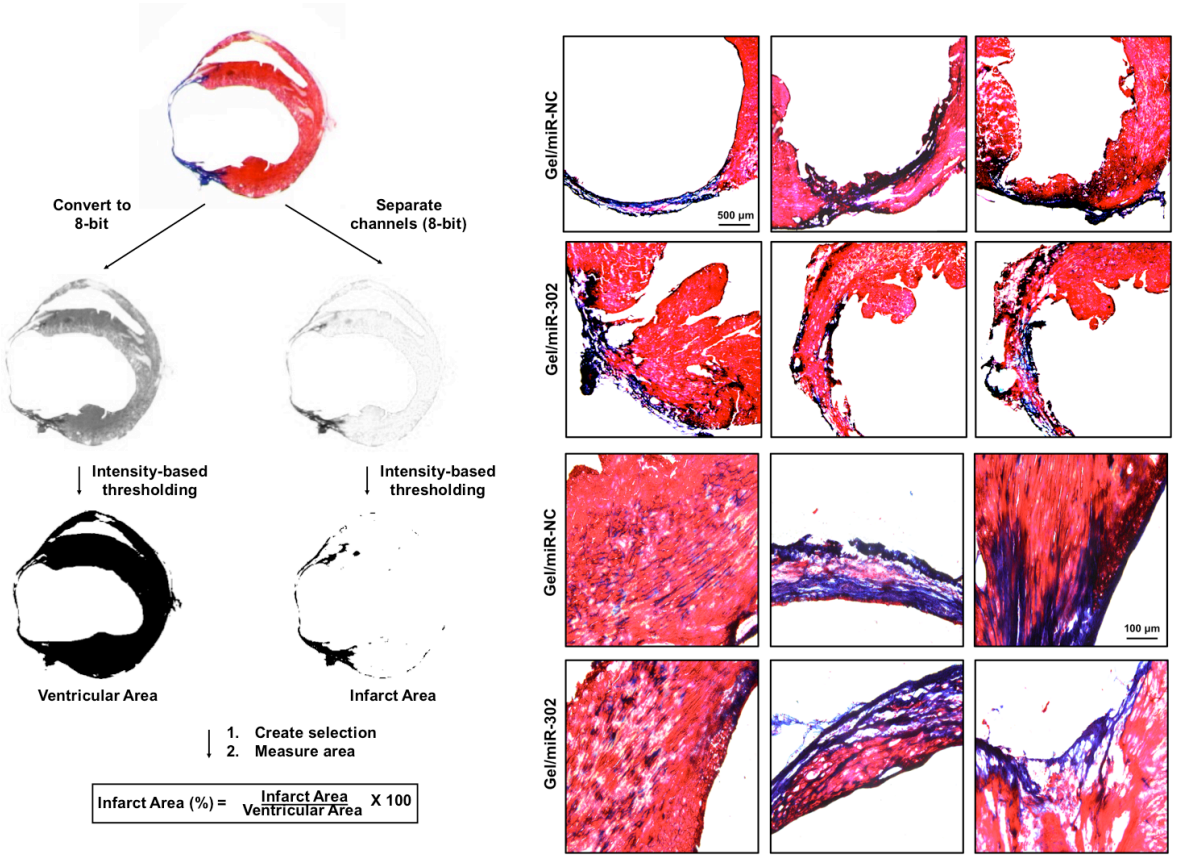

Supplementary Figure 15. Method for ImageJ quantification of infarct size and representative hi-magnification Masson's images. Infarct size was quantified using threshold analysis on ImageJ from separate channels and manual thresholding to separate infarct from non-infarcted tissue. Representative sections at low and high magnification of gel/miR-NC and gel/miR-302 treated hearts at 28 days are shown.

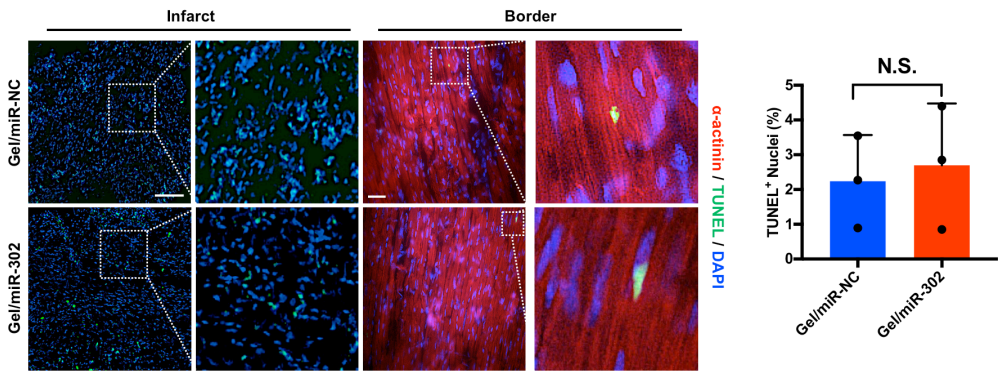

Supplementary Figure 16. Apoptosis in gel/miR-NC or gel/miR-302 treated sections after MI. Following infarction and gel/miR-302 or gel/miR-NC treatment, mice were sacrificed at D28 and hearts were explanted and processed for IHC. TUNEL was used to stain for apoptosis in the site of infarct and α-actinin was used to stain cardiomyocytes and to delineate infarct tissue. No significant differences were found in TUNEL staining. Scale bar infarct = 100 μM, scale bar border = 50 μM (mean ± SD, n=3 mice per group, N.S. = not significant).

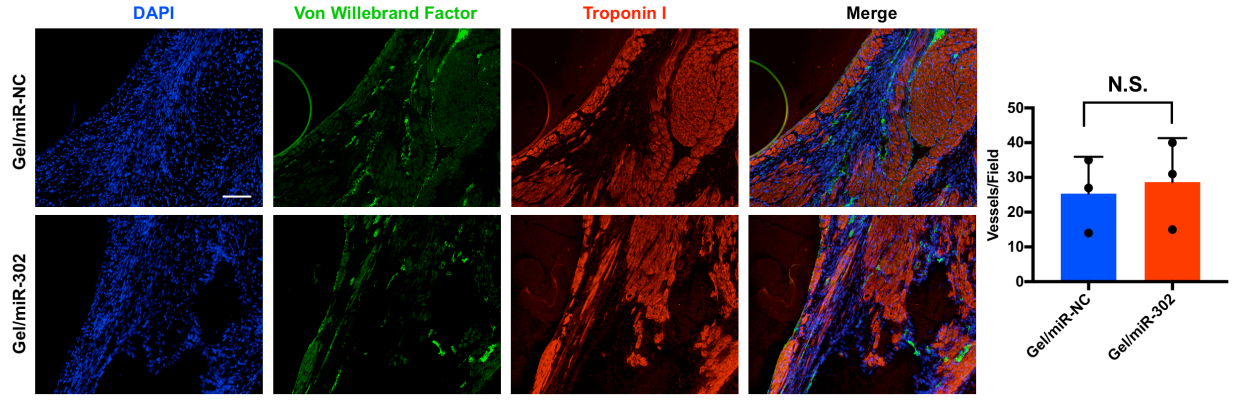

Supplementary Figure 17. Vascular density 28 days after MI. Following infarction and gel/miR-302 or gel/miR-NC treatment, mice were sacrificed at D28 and hearts were explanted and processed for IHC. Sections were stained with cardiac Troponin I to mark cardiomyocytes, or von Willebrand Factor (vWF) to mark endothelium. There was no significant difference in vascular density in gel/miR-NC or gel/miR-302 treated mice in infarct tissue. vWF quantification was performed in the infarct size on all vessels larger than 5 μm. Scale bar = 100 μm (mean ± SD, n=3 mice per group, N.S. = not significant).

References:

1. Rodell, C. B., Kaminski, A. L. & Burdick, J. A. Rational Design of Network Properties in Guest–Host Assembled and Shear-Thinning Hyaluronic Acid Hydrogels. *Biomacromolecules* **14,** 4125–4134 (2013).
2. Tian, Y. *et al.* A microRNA-Hippo pathway that promotes cardiomyocyte proliferation and cardiac regeneration in mice. *Sci. Transl. Med.* **7,** 279ra38 (2015).
3. Rodell, C. B. *et al.* Shear-Thinning Supramolecular Hydrogels with Secondary Autonomous Covalent Crosslinking to Modulate Viscoelastic Properties In Vivo. *Adv. Funct. Mater.* **25,** 636–644 (2014).